Earth and Planetary Science Letters 429 (2015) 33–44

Contents lists available at ScienceDirect

Earth and Planetary Science Letters

www.elsevier.com/locate/epsl

Paleogene plants fractionated carbon isotopes similar to modern plants

Aaron F. Diefendorf[a,*], Katherine H. Freeman[b], Scott L. Wing[c], Ellen D. Currano[d], Kevin E. Mueller[e]

[a] Department of Geology, University of Cincinnati, PO Box 210013, Cincinnati, OH 45221-0013, USA
[b] Department of Geosciences, The Pennsylvania State University, University Park, PA 16802, USA
[c] Department of Paleobiology, NHB121, P.O. Box 37012, Smithsonian Institution, Washington, DC 20013, USA
[d] Department of Botany, University of Wyoming, 1000 E University Ave, Laramie, WY 82071, USA
[e] U.S. Department of Agriculture, Agricultural Research Service, Rangeland Resources Research Unit, Fort Collins, CO 80526, USA

ARTICLE INFO

Article history:
Received 8 January 2015
Received in revised form 9 July 2015
Accepted 14 July 2015
Available online xxxx
Editor: H. Stoll

Keywords:
Paleocene
Eocene
bighorn basin
biomarkers
lipids
compound specific isotope analyses

ABSTRACT

The carbon isotope composition ($\delta^{13}C$) of terrestrial plant biomarkers, such as leaf waxes and terpenoids, provides insights into past carbon cycling. The $\delta^{13}C$ values of modern plant biomarkers are known to be sensitive to climate and vegetation type, both of which influence fractionation during lipid biosynthesis by altering plant carbon supply and its biochemical allocation. It is not known if fractionation observed in living plants can be used to interpret fossil lipids because plant biochemical characteristics may have evolved during the Cenozoic in response to changes in global climate and atmospheric CO_2. The goal of this study was to determine if fractionation during photosynthesis (Δ_{leaf}) in the Paleogene was consistent with expectations based on living plants. To study plant fractionation during the Paleogene, we collected samples from eight stratigraphic beds in the Bighorn Basin (Wyoming, USA) that ranged in age from 63 to 53 Ma. For each sample, we measured the $\delta^{13}C$ of angiosperm biomarkers (triterpenoids and *n*-alkanes) and, abundance permitting, conifer biomarkers (diterpenoids). Leaf $\delta^{13}C$ values estimated from different angiosperms biomarkers were consistently 2‰ lower than leaf $\delta^{13}C$ values for conifers calculated from diterpenoids. This difference is consistent with observations of living conifers and angiosperms and the consistency among different biomarkers suggests ancient ε_{lipid} values were similar to those in living plants. From these biomarker-based $\delta^{13}C_{leaf}$ values and independent records of atmospheric $\delta^{13}C$ values, we calculated Δ_{leaf}. These calculated Δ_{leaf} values were then compared to Δ_{leaf} values modeled by applying the effects that precipitation and major taxonomic group in living plants have on Δ_{leaf} values. Calculated and modeled Δ_{leaf} values were offset by less than a permil. This similarity suggests that carbon fractionation in Paleogene plants changed with water availability and major taxonomic group to about the same degree it does today. Further, paleoproxy data suggest at least two of the stratigraphic beds were deposited at times when pCO_2 levels were higher than today. Biomarker data from these beds are not consistent with elevated Δ_{leaf} values, possibly because plants adapted carbon uptake and assimilation characteristics to pCO_2 changes over long timescales.

© 2015 Elsevier B.V. All rights reserved.

1. Introduction

Terrestrial plant biomarkers, and their carbon isotope ratios ($\delta^{13}C$), provide insights into ecosystems and carbon cycling from local to global scales (e.g., McInerney and Wing, 2011; Bowen, 2013). Considerable efforts have been made to constrain carbon sources, fluxes and fates, especially during periods of rapid climate change, such as hyperthermal events at the beginning of the Eocene (cf., McInerney and Wing, 2011; Bowen, 2013). Carbon isotope excursions (CIEs) during critical time intervals, such as during the Paleocene–Eocene Thermal Maximum, provide similar records of CIE shape and direction at different sites, but the CIE magnitude and shape differ, causing uncertainty in the size and timing of the carbon perturbation. This disagreement among records has led to questions about the degree to which local records of $\delta^{13}C$ record shifts in the isotopic composition of the atmosphere (e.g., McInerney and Wing, 2011). It also implies plant $\delta^{13}C$ records have variable sensitivities to changing climate and plant communities (Diefendorf et al., 2010).

Changes in the $\delta^{13}C$ of terrestrial organic matter (and especially plant biomarkers) through geologic time are often used as proxies for atmospheric $\delta^{13}C$, because having been fixed from atmospheric

* Corresponding author. Tel.: +1 513 556 3787.
E-mail address: aaron.diefendorf@uc.edu (A.F. Diefendorf).

http://dx.doi.org/10.1016/j.epsl.2015.07.029
0012-821X/© 2015 Elsevier B.V. All rights reserved.

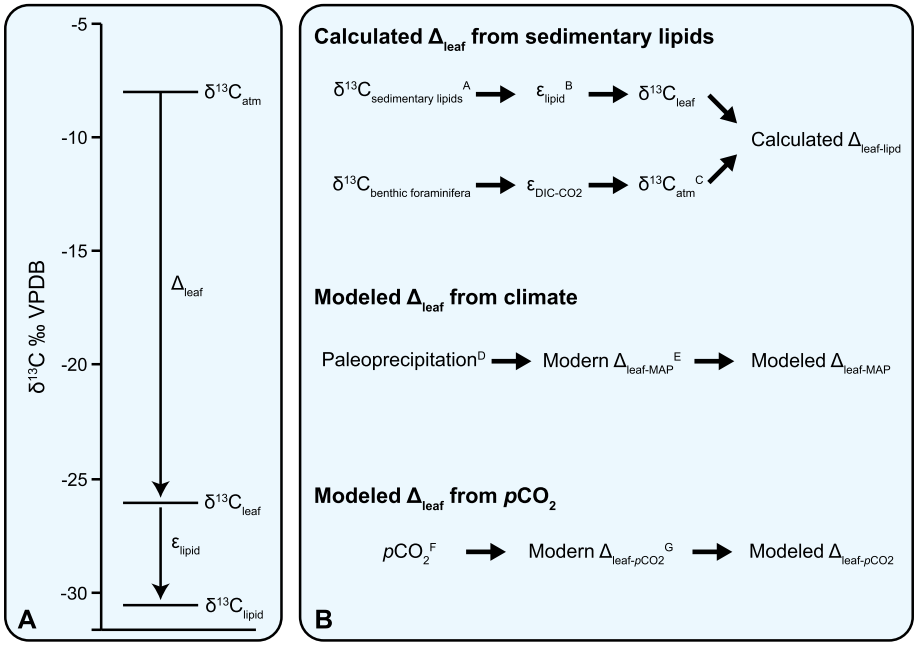

Fig. 1. A) Lipids and their carbon isotope ($\delta^{13}C_{lipid}$) values are preserved in the geologic record and provide a link to leaf $\delta^{13}C$ ($\delta^{13}C_{leaf}$), after constraining for fractionation that occurs during lipid biosynthesis (ε_{lipid}), or to atmospheric CO_2 $\delta^{13}C$ values ($\delta^{13}C_{atm}$), after constraining for fractionation that occurs during photosynthesis (Δ_{leaf}). Alternatively, Δ_{leaf} can be calculated if $\delta^{13}C_{atm}$ is known, and this provides a measure of discrimination which can be useful for interpreting water availability, ecophysiology, vegetation information, etc. (see text for details). B) In this study, Δ_{leaf} is calculated (calculated $\Delta_{leaf\text{-}lipid}$) from sedimentary lipid $\delta^{13}C$ values, after controlling for fractionation during lipid biosynthesis and using $\delta^{13}C_{atm}$ values derived from benthic foraminifera. Calculated $\Delta_{leaf\text{-}lipid}$ values are then compared to modeled Δ_{leaf} values based on modern plant studies. Δ_{leaf} values are modeled for both angiosperms and conifers using modern relationships between Δ_{leaf} and plant type and paleoprecipitation (modeled $\Delta_{leaf\text{-}MAP}$). Also, Δ_{leaf} values are modeled for angiosperms using modern Δ_{leaf} relationships between Δ_{leaf} and pCO_2. The various sources of inputs are as follows: [A] This study; [B] Diefendorf et al. (2011, 2012); [C] Tipple et al. (2010); [D] Currano et al. (2008, 2010); [E] Diefendorf et al. (2010); [F] Beerling and Royer (2011); [G] Schubert and Jahren (2012).

CO_2 through photosynthesis, plant carbon should reflect the $\delta^{13}C$ of the atmosphere. This process assumes that the many sources of fractionation between atmosphere and plant are constant or can be corrected for (Diefendorf et al., 2010; Freeman et al., 2011; Cernusak et al., 2013). During carbon fixation, atmospheric CO_2 is converted to sugars by the enzyme Rubisco, which fractionates strongly against ^{13}C; this enzymatic discrimination, along with other factors (diffusion, mesophyll and stomatal conductance), results in a large net isotope effect (e.g., Farquhar et al., 1989). Fractionation during photosynthesis (Δ_{leaf}), also referred to as carbon isotope discrimination, is quantified as

$$\Delta_{leaf} = \frac{\delta^{13}C_{atm} - \delta^{13}C_{leaf}}{1 + (\delta^{13}C_{leaf}/1000)} \quad (1)$$

Theoretical and empirical studies show that fractionation during carbon assimilation and fixation is sensitive to many factors including water availability, major taxonomic group, light intensity, photosynthetic pathway, and carbon dioxide partial pressure (Farquhar et al., 1989; Diefendorf et al., 2010; Schubert and Jahren, 2012; Cernusak et al., 2013; Graham et al., 2014).

For studies using lipid biomarkers, carbon isotope fractionation during biomarker synthesis is also important (Fig. 1A), but it is less constrained than photosynthetic fractionation. Isotope fractionation occurs during biochemical reactions and the net fractionation is a function of carbon source, the availability of the reactant, and down-stream reactions that influence fractionation (Hayes, 2001). Fractionation during biosynthesis (ε_{lipid}) is quantified by:

$$\varepsilon_{lipid} = \left(\frac{\delta^{13}C_{lipid} + 1000}{\delta^{13}C_{leaf} + 1000} - 1\right) \times 10^3 \approx \left(\delta^{13}C_{lipid} - \delta^{13}C_{leaf}\right) \quad (2)$$

The purpose of this study was to improve our ability to interpret past changes in carbon isotope composition of land plant biomarkers by establishing if Δ_{leaf} was different during the Paleogene when climate and atmospheric conditions deviated, sometimes greatly, from modern conditions. To accomplish our goal, we focused on sediments collected from the Paleocene (63 Ma) to early Eocene (53 Ma) from the Bighorn Basin (Wyoming, USA). This area was chosen because of the detailed climate and floral information that has been the focus of many studies. Samples were collected from eight stratigraphic beds, with multiple horizons sampled from within beds, yielding fifteen horizons. A companion study focused on terpenoid biomarkers as fossil vegetation proxies (Diefendorf et al., 2014). We measured $\delta^{13}C$ values of leaf wax *n*-alkanes, one of the most commonly used biomarkers, and di- and triterpenoids that are specific to conifers and angiosperms, respectively, from the same rocks samples. Although terpenoid compounds are not as well preserved as *n*-alkanes (Diefendorf et al., 2014), they provide unaltered taxon-specific $\delta^{13}C$ values (Freeman et al., 1994). We measured them in this study to compare conifers and angiosperms, which are known to have different Δ_{leaf} values when grown under similar conditions (see Diefendorf et al., 2010; 2011 and references therein).

We calculated Δ_{leaf} values from the $\delta^{13}C$ values of individual plant biomarkers ($\Delta_{leaf\text{-}lipid}$; Fig. 1B), after correcting for biosynthetic fractionation, and from estimates of $\delta^{13}C_{atm}$ based on benthic foraminifera (Tipple et al., 2010). These calculated $\Delta_{leaf\text{-}lipid}$ values were then compared to estimated, or "modeled", Δ_{leaf} values that were determined using two approaches (Fig. 1B). The first approach, denoted as $\Delta_{leaf\text{-}MAP}$, models Δ_{leaf} values as a function of the potential effects of precipitation on Δ_{leaf}, following a meta-analysis of Δ_{leaf} values from 334 living woody plant species that also accounts for effects of major taxonomic group on Δ_{leaf} (i.e. it

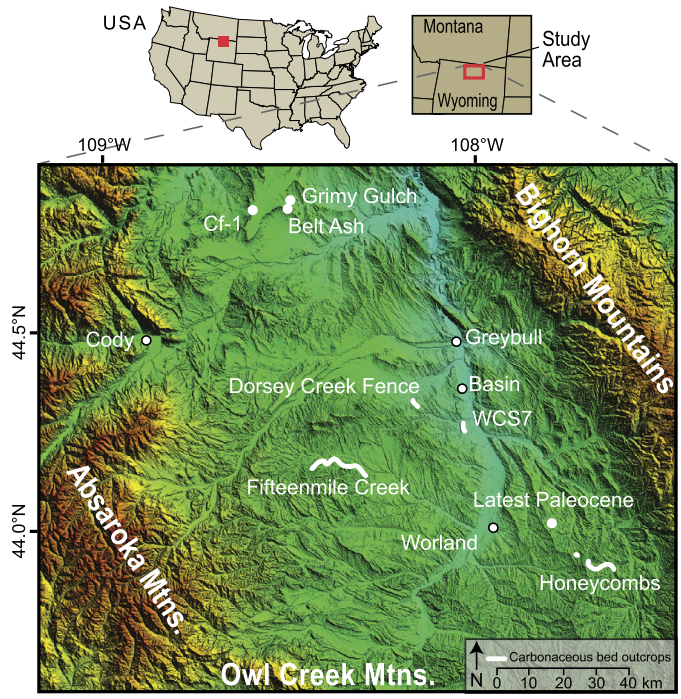

Fig. 2. Location of the Bighorn Basin within the USA and location of sampling sites within the Bighorn Basin. (For interpretation of the references to color in this figure, the reader is referred to the web version of this article.)

considered angiosperms and gymnosperms separately; Diefendorf et al., 2010). The second approach, denoted as $\Delta_{\text{leaf-}pCO_2}$, models Δ_{leaf} values as a function of atmospheric pCO_2 on Δ_{leaf}, following a study of two living plant species described by Schubert and Jahren (2012). To determine if Δ_{leaf} variability during the Paleogene is consistent with the effects of environmental conditions and plant phylogeny on Δ_{leaf} of living plants, we then compared calculated and modeled Δ_{leaf} values. We conclude that Paleogene plants are likely to have had similar Δ_{leaf} to living plants, and that including the effect of precipitation and taxonomic group increases the correspondence between Paleogene Δ_{leaf} and modern Δ_{leaf}. We do not find evidence that Δ_{leaf} is influenced by pCO_2 during the Paleogene.

2. Sample locations and methods

2.1. Geological and sedimentological setting

Samples were collected from outcrops of the Paleocene Fort Union and lower Eocene Willwood Formations in the Bighorn Basin, Wyoming, USA (Fig. 2). The Bighorn Basin is a Laramide structural depression surrounded by mountains uplifted during the Paleocene and early Eocene (Bown, 1980). Common lithologies include fluvial sandstones, mudstones, minor lignites and carbonaceous shales (i.e. organic carbon rich). Fort Union sediments are primarily gray-brown colored with interspersed lignitic and carbonaceous shales (Bown, 1980). The Willwood Formation is dominated by oxidized mudstone paleosols that are variegated red, purple, and yellow, but there are also channel sandstones, laterally extensive carbonaceous shales and abandoned channel deposits containing plant fossils and dispersed organic material (e.g., Davies-Vollum and Wing, 1998). The paleoelevation of the Bighorn Basin during the Paleogene was likely <1 km (Wing and Greenwood, 1993; McMillan et al., 2006).

The age of each bed was calculated by linear interpolation between levels of known age and stratigraphic position within each section (Wing et al., 2000; Wing and Currano, 2013). Each sampled stratigraphic level is a laterally continuous (ca. 0.5 to 18 km) carbonaceous bed. These carbonaceous beds represent deposition on wet distal floodplains where organic matter (OM) was preserved because of a high water table, reducing conditions in the sediment and frequent depositional events. Individual carbonaceous beds are thought to represent deposition over a period of centuries to a few millennia (Davies-Vollum and Wing, 1998). Bed descriptions, age determination, and flora are reported in Diefendorf et al. (2014).

Within each carbonaceous bed, samples were collected from five sites spaced at intervals of hundreds of meters along the outcrop, and at each site one to three different lithologies (horizons) were collected from unweathered rock dug from a short vertical section through the bed (Table 1). For each sample, we measured the proportion (wt.%) of total organic carbon (TOC) and the carbon isotope value of TOC ($\delta^{13}C_{TOC}$; $n = 75$). A subset of samples was selected for biomarker analysis ($n = 43$).

2.2. Extraction and separation

Samples for extraction were rinsed with dichloromethane (DCM), broken into ca. 1-cm pieces, oven-dried and powdered in a ball mill. Powdered samples (25–120 g) were extracted by Soxhlet with DCM/methanol (9:1, v/v) for 24 h. The total lipid extract was purified via asphaltene precipitation and separated into apolar and polar fractions on silica gel with hexanes/DCM (9:1, v/v) and DCM/MeOH (1:1), respectively. The apolar fraction was further separated into saturated and unsaturated fractions on 5% Ag-impregnated silica gel (w/w) with hexanes and ethyl acetate, respectively.

2.3. Identification and quantification

Lipids were assigned using gas chromatography-mass spectrometry (GC-MS) with a Hewlett–Packard (HP) 6890 GC instrument coupled to an HP 5973 quadrupole MS with electron ionization. A fused silica column (Agilent J&W DB-5; 30 m, 0.25 mm, 25 µm) was used. A split/splitless injector was operated in pulsed splitless mode at 320 °C with a column flow of 1.5 ml/min. The temperature program was: 60 °C (1 min) to 140 °C at 15 °C/min, then to 320 °C (held 20 min) at 4 °C/min.

2.4. Bulk carbon isotope analyses

$\delta^{13}C$ of bulk organic carbon and weight percent total organic carbon (wt.% TOC) were determined via continuous flow (He; 120 ml/min) on a Costech elemental analyzer (EA) coupled to a Thermo Finnegan Delta Plus XP IRMS. $\delta^{13}C$ values were corrected for sample size dependency and then normalized to the VPDB scale using a two-point calibration. Error was determined by analyzing additional independent standards measured in all EA runs. Long-term accuracy of all EA runs was ±0.01‰ ($n = 116$) and precision was ±0.12‰ ($n = 170$; 1σ).

2.5. Compound-specific carbon isotope analyses

Saturated and unsaturated hydrocarbon fractions were analyzed on a Varian model 3400 GC coupled to a Finnegan Mat 252 IRMS. Isotopic abundances were determined relative to a reference gas calibrated with Mix A (n-C_{16} to n-C_{30} alkanes; Arndt Schimmelmann; Indiana University). Within run precision and accuracy was determined with co-injected internal standards and are 0.18‰ (1σ, $n = 153$) and −0.08‰ ($n = 153$), respectively. Mix A was analyzed daily to verify long-term stability of the reference gas calibration.

Table 1
Bed names, stratigraphic and age information, paleovegetation and paleoclimate.

Bed name	Level m (section)[a]	Epoch	Formation	Age (Ma)	Conifer pale-ovegetation (%)[b]	MAP (cm), ±1SE[c]	MAT (°C)[d]	pCO_2 (ppmV), ±1σ[f]	$\delta^{13}C_{atm}$ (‰), ±90%CI[g]
Fifteenmile Creek	700 m (ECS)	Eocene	Willwood	52.98	3 to 9	114 (+49, −34)	22.2 ± 2.0	946 ± 633	−5.8 ± 0.4
Dorsey Creek Fence	353 m (ECS)	Eocene	Willwood	54.37	≤5	132 (+57, −40)	10.8 ± 3.3	456 ± 171	−5.3 ± 0.4
WCS7	112 m (ECS)	Eocene	Willwood	55.34	≤5	173[e]	16.4 ± 2.7	394 ± 153	−5.0 ± 0.4
Latest Paleocene	7.5 m below CIE	Paleocene	Fort Union	56.04	≤5	173 (+75, −52)	16.4 ± 2.9	405 ± 162	−4.7 ± 0.4
Honeycombs	13 m below CIE	Paleocene	Fort Union	56.1	≤14	173[e]	16.4 ± 2.9	405 ± 162	−4.7 ± 0.4
Cf-1	429 m (WPB)	Paleocene	Fort Union	57.39	≤5	109 (+47, −33)	12.0 ± 2.9	451 ± 167	−4.2 ± 0.4
Belt Ash	351 m (SPB)	Paleocene	Fort Union	59.39	≤5	120 (+52, −36)	10.5 ± 2.9	564 ± 26	−4.7 ± 0.4
Grimy Gulch	56 m (SPB)	Paleocene	Fort Union	63	≤5	120[e]	n.d.	361 ± 42	−5.5 ± 0.4

[a] ECS, Elk Creek Section; CIE, Paleocene–Eocene Thermal Maximum Carbon Isotope Excursion; WPB, West Polecat Bench; SPB, Southeast Polecat Bench.
[b] Paleovegetation estimated from previous floral studies in the Bighorn Basin (see Diefendorf et al., 2014).
[c] Mean annual precipitation (MAP) estimates from leaf-area analysis of previously collected leaf specimens and their associated errors (Currano et al., 2008, 2010).
[d] MAP values for WCS7 and Honeycombs were approximated with samples collected from the Latest Paleocene site and Grimy Gulch samples were approximated with values from the Belt Ash. Although sample collections precluded leaf-area calculations (insufficient plant species), sample lithology and flora are consistent with a wet depositional environment.
[e] Mean annual temperature (MAT) estimates (Wing et al., 2000; Currano et al., 2008, 2010).
[f] Atmospheric carbon dioxide concentrations and standard deviations from Beerling and Royer (2011) and averaged for a 3 Ma time step for consistency with $\delta^{13}C_{atm}$ values.
[g] Carbon isotope values of atmospheric carbon dioxide as determined from benthic foraminifera and averaged using a 3 Ma time step (Tipple et al., 2010).

2.6. Statistical analyses and Monte Carlo method

All statistical analyses were performed using JMP Pro 11.0 (SAS, Cary, USA). Uncertainties for all Δ_{leaf} values were determined using the Monte Carlo method (Anderson, 1976) with 3000 iterations. This was sufficient replication for the Monte Carlo standard error of the mean to be less than 0.1‰. Input uncertainties were considered for $\delta^{13}C_{atm}$ and pCO_2, mean annual precipitation (MAP), $\delta^{13}C$ values of *n*-alkanes and terpenoids, lipid biosynthetic fractionation (ε_{lipid}), and uncertainties in Δ_{leaf} models from Diefendorf et al. (2010).

3. Results

3.1. Description and organic geochemistry of sediments

All sediments were deposited in wet floodplain environments, but variations in grain size, TOC and sedimentary features indicate a range of sub-habitats (Wing, 1984). Local heterogeneity in the composition of leaf fossil assemblages along each bed indicates variability in the ancient vegetation (Davies-Vollum and Wing, 1998), and this variability is also observed in the spatial distributions of biomarkers. Biomass estimates from leaf assemblages are dominated by angiosperms (85–95% of the total flora; see Diefendorf et al., 2014).

The *n*-alkane concentrations were highest for long-chain *n*-alkanes (e.g. C_{27} to C_{33}) derived from vascular plant leaf wax (Fig. 3). The most abundant was *n*-C_{29} with a concentration ranging from 0 to 285 μg/g C (mean 54 μg/g C). Long-chain *n*-alkane abundances were highest for samples from Fifteenmile Creek and the Latest Paleocene. Mid-chain *n*-alkanes, produced in relatively large quantities by submerged and floating aquatic plants, were typically lower in abundance (mean of 15 μg/g C) than long-chain *n*-alkanes. Short-chain *n*-alkanes, typical of algae (C_{15}, C_{17}, C_{19}), had the lowest abundance (5 μg/g C). The higher abundance of longer chain *n*-alkanes is typical of terrestrial sediments, where the dominant source of *n*-alkanes is higher plants, with a minor contribution from aquatic sources (Diefendorf et al., 2014). Sediment lithologies sampled in this study (shales, lignites and mudstones) are typical of overbank facies associated with aggrading fluvial systems (Jones and Hajek, 2007). As a result, the amount of aquatic OM varied. This is supported by variable abundances of short-chain *n*-alkanes in the sediments (Diefendorf et al., 2014). The *n*-alkane average chain length (ACL) ranged between 27.4 and 29.3 (Diefendorf et al., 2014) and is within the range commonly observed for modern tree species (Diefendorf et al., 2011; Bush and McInerney, 2013).

Plant-derived terpenoids were present in all but one of the samples (Fig. 3). Conifer-derived tricyclic diterpenoids were found in the saturated and unsaturated hydrocarbon fractions with the most abundant diterpenoids in the pimarane and abietane classes. Angiosperm-derived pentacyclic triterpenoids were also abundant (Diefendorf et al., 2014).

3.2. Bulk carbon isotopes

$\delta^{13}C_{TOC}$ values range from −23.5 to −28.2‰ (Table 2 and A-1, Fig. 4). Within each stratigraphic horizon, $\delta^{13}C_{TOC}$ ranges were smaller, but still highly variable. For example, $\delta^{13}C_{TOC}$ values in lignitic shales varied from −23.5 to −26.2‰ at Cf-1 and from −25.6 to −27.7‰ at the Honeycombs. Standard deviations of $\delta^{13}C_{TOC}$ values within each stratigraphic horizon range from 0.2 to 1.1‰ (Table 2). Weight % TOC varied from 0.1 to 55.9%. Contrary to previous studies of these formations (Wing et al., 2005), no correlation was observed between weight % TOC and $\delta^{13}C_{TOC}$ ($R^2 = 0.02$, $p = 0.19$), even if only samples with <4% TOC were considered.

3.3. Compound-specific carbon isotopes

Carbon isotope values of long-chain *n*-alkanes (Fig. 4, Table 3 and A-1) are slightly different between chain lengths. For the *n*-C_{29} alkane, values ranged between −32.9‰ at Grimy Gulch and −28.9‰ at the Belt Ash. Values typically ranged c. 1.7‰ for multiple samples collected from the same stratigraphic bed with standard deviations ranging from 0.3 to 1.0‰.$\delta^{13}C$ values of tricyclic diterpenoids ranged from −30.0‰ at the Latest Paleocene to −21.9‰ at the Belt Ash. Dehydroabietane, a common terpenoid found in geologic samples and the most common diterpenoid in this study, ranged from −25.9 to −20.3‰. Triterpenoid $\delta^{13}C$ values ranged from −28.8 to −25.8‰. The most common triterpenoids, 2,2,4a,9-tetramethyl-1,2,3,4,4a,5,6,14b-octahydropicene and des-A-lupane, ranged from −28.9 to −24.6‰ and −28.3 to −25.6‰, respectively. Diterpenoids were 1.7‰ higher than triterpenoids ($n = 14$, paired *t*-test, $p = 0.02$) measured in the same

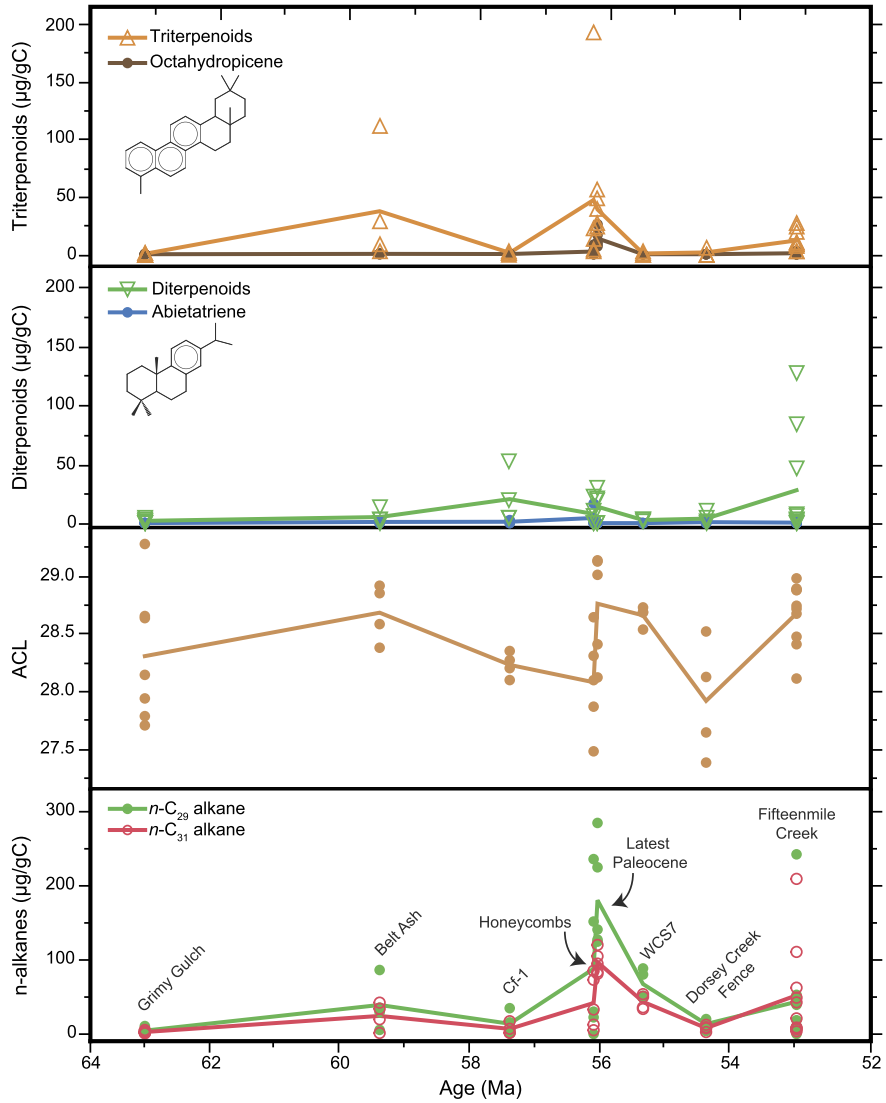

Fig. 3. Selected geochemical data including total *n*-alkane concentrations, average chain length (ACL), diterpenoid concentrations for all compounds and for abietatriene (structure shown), and triterpenoid concentrations for all compounds and for 2,2,4a,9-Tetramethyl-1,2,3,4,4a,5,6,14b-octahydropicene (structure shown) for all stratigraphic beds. See Diefendorf et al. (2014) for additional geochemical data.

Table 2
Bulk carbon isotopes and weight percent total organic carbon by stratigraphic bed.

Bed name	Age (Ma)	Lithology	Position along stratigraphic level					$\delta^{13}C_{TOC}$ mean	1σ
			1	2	3	4	5		
			$\delta^{13}C_{TOC}$‰ VPDB (wt.% TOC)						
Fifteenmile Creek	52.98	Lignitic shale/clayey mudstone	−28.1 (1.9)	−27.5 (17.2)	−27.4 (25.0)	−27.8 (46.0)	−28.2 (14.8)	−27.8	0.3
		Clayey Mudstone	−26.8 (8.5)	−28.0 (1.7)	−27.5 (2.9)	−27.9 (2.9)	−27.7 (12.1)	−27.6	0.4
Dorsey Creek Fence	54.37	Carb. shale	−26.8 (20.3)	−26.1 (47.1)	−26.4 (7.6)	−26.8 (1.9)	−26.3 (4.9)	−26.5	0.3
		Clayey mudstone	−25.7 (0.1)	−25.3 (0.1)	−26.5 (0.5)	−25.3 (0.2)	−25.5 (0.1)	−25.7	0.5
WCS7	55.34	Carb. shale	−26.5 (0.6)	−26.5 (0.8)	−27.0 (0.8)	−26.5 (0.7)	−26.9 (0.9)	−26.7	0.3
		Mudstone	−26.2 (2.4)	−26.8 (1.0)	−26.6 (0.6)	−26.7 (0.7)	−27.3 (1.1)	−26.7	0.4
Latest Paleocene	56.04	Silt/sandstone	−26.6 (0.6)	−25.7 (0.6)	−26.2 (0.9)	−26.1 (1.0)	−25.9 (0.9)	−26.1	0.3
Honeycombs	56.1	Clayey mud/siltstone	−25.9 (16.9)	−25.6 (0.9)	−26.9 (1.1)	−27.7 (1.4)	−27 (26.1)	−26.6	0.9
Cf−1	57.39	Carb. mudstone/shale	−25.6 (2.1)	−25.5 (2.5)	−25.3 (1.8)	−25.2 (3.5)	−25.5 (3.4)	−25.4	0.2
		Lignitic shale	−26.2 (49.3)	−25.4 (44)	−26.0 (38.3)	−23.5 (55.6)	−26.0 (29.9)	−25.4	1.1
Belt Ash	59.39	Carb. mudstone/shale	−25.1 (3.9)	−25.8 (3.0)	−24.6 (2.0)	−25.5 (1.2)	−25.0 (1.6)	−25.2	0.5
		Lignitic shale	−25.9 (14.3)	−26.2 (23.0)	−24.4 (28.9)	−26.3 (35.5)	−25.8 (30.1)	−25.7	0.8
Grimy Gulch	63	Carb. mudstone/shale	−24.8 (3.1)	−24.8 (7.7)	−24.9 (3.4)	−25.2 (0.8)	−25.2 (4.4)	−25.0	0.2
		Lignite	−25.7 (54.6)	−24.8 (48.2)	−25.5 (54.3)	−25.2 (55.9)	−24.9 (47.4)	−25.2	0.4
		Carb. Mudstone	−24.7 (1.2)	−25.1 (3.1)	−24.8 (3.3)	−25.4 (1.5)	−24.8 (2.5)	−25.0	0.3

samples. Compared to n-C_{29} alkane as measured in the same samples, diterpenoids were 6.0‰ higher ($n = 25$, Wilcoxon Signed Rank, $p < 0.0001$) and triterpenoids were 4.1‰ higher ($n = 21$, paired t-test, $p < 0.0001$). These comparisons of $\delta^{13}C$ values of terpenoids and n-alkanes do not take into account differences in biosynthetic fractionation at this level (see below).

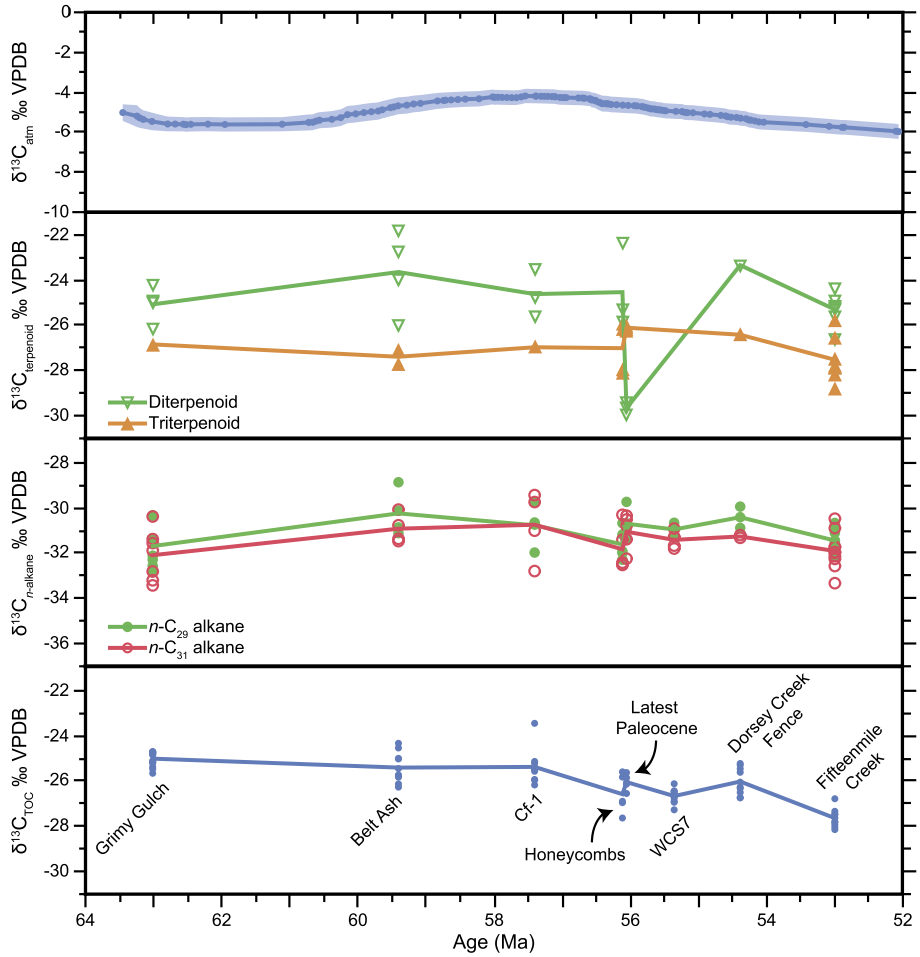

Fig. 4. Total organic carbon (TOC), lipid and atmospheric $\delta^{13}C$ data for all stratigraphic beds. $\delta^{13}C_{atm}$ values are from Tipple et al. (2010) and are shown with the reported 90% confidence interval.

Table 3
Measured bulk and compound-specific *n*-alkane, diterpenoid, and triterpenoid carbon isotope values by stratigraphic bed.

Bed name	Age (Ma)	$\delta^{13}C_{TOC}$	1σ	N	$\delta^{13}C$ n-C_{29}	1σ	N	$\delta^{13}C$ n-C_{31}	1σ	N	$\delta^{13}C$ di.	1σ	N	$\delta^{13}C$ tri.	1σ	N
Fifteenmile Creek	52.98	−27.7	0.4	10	−31.5	0.5	10	−31.9	0.8	10	−25.3	0.7	7	−27.6	1.0	8
Dorsey Creek Fence	54.37	−26.1	0.6	10	−30.4	0.5	3	−31.3	0.1	2	−23.4	n.a.	1	−26.5	n.a.	1
WCS7	55.34	−26.7	0.3	10	−31.0	0.3	4	−31.4	0.4	4	n.a.	n.a.	0	n.a.	n.a.	0
Latest Paleocene	56.04	−26.1	0.3	5	−30.7	0.6	5	−31.1	0.8	5	−29.7	0.3	3	−26.1	0.1	4
Honeycombs	56.1	−26.6	0.9	5	−31.6	0.7	5	−31.9	1.0	5	−24.6	1.9	3	−27.0	1.1	4
Cf-1	57.39	−25.4	0.8	10	−30.8	0.9	4	−30.8	1.5	4	−24.7	1.1	3	−27.0	n.a.	1
Belt Ash	59.39	−25.4	0.7	10	−30.3	1.0	4	−31.0	0.6	4	−23.7	1.8	4	−27.4	0.4	2
Grimy Gulch	63	−25.1	0.3	15	−31.7	1.0	7	−32.1	1.1	7	−25.1	0.8	4	−26.9	n.a.	1

3.4. *Paleogene leaf $\delta^{13}C$ values*

Lipid $\delta^{13}C$ values were converted to leaf $\delta^{13}C$ values ($\delta^{13}C_{leaf}$) using a correction for the net fractionation during lipid biosynthesis (ε_{lipid}). Both the biochemical pathways and their characteristic ε_{lipid} values vary by lipid class. In the case of *n*-alkanes, fractionation occurs during the conversion of pyruvate to acetyl-CoA to yield *n*-alkanoic acids of intermediate length, which are subsequently elongated, and then decarboxylated to *n*-alkanes (Kolattukudy et al., 1976). Based on analyses of modern angiosperm trees in the temperate zone, ε_{lipid} values for *n*-alkanes average −4.6‰ (±2.2, 1σ) and −5.0‰ (±2.2, 1σ) for n-C_{29} and n-C_{31}, respectively (Diefendorf et al., 2011), but see Discussion Section 4.1.

Terpenoids biosynthesis, which can take place by several pathways, characteristically differs among plant types. Conifers synthesize diterpenoids by the 2-C-methyl-D-erythritol-4-phosphate (MEP) pathway, while angiosperms synthesize triterpenoids by the mevalonic acid (MVA) pathway. Although environmental, functional and taxonomic controls on terpenoid biosynthetic fractionation are not known, ε_{lipid} values observed in living plants are much smaller for both types of terpenoids relative to *n*-alkanes. For the species studied thus far, including conifers and angiosperm tree species from the temperate zone, ε_{lipid} values are −0.6‰ (±1.8, 1σ) and −0.4‰ (±1.2, 1σ) for diterpenoids and triterpenoids, respectively (Diefendorf et al., 2012).

Leaf $\delta^{13}C$ values were calculated using ε_{lipid} values reported above (Table 4) and Equation (2). $\delta^{13}C_{leaf}$ values were similar, despite being calculated separately from n-C_{29} alkanes and triterpenoids ($n = 25$, paired t-test). This similarity is notable, and is consistent with previous work that suggests the *n*-alkanes are pri-

Table 4
Calculated leaf $\delta^{13}C$ values for *n*-alkanes, diterpenoids, and triterpenoids by stratigraphic bed.

Bed name	Age (Ma)	Angiosperms			Conifers
		$\delta^{13}C_{leaf(n\text{-}C_{29})}$	$\delta^{13}C_{leaf(n\text{-}C_{31})}$	$\delta^{13}C_{leaf(triterpenoids)}$	$\delta^{13}C_{leaf(diterpenoids)}$
Fifteenmile Creek	52.98	−27.0	−27.1	−27.2	−24.8
Dorsey Creek Fence	54.37	−26.0	−26.4	−26.1	−22.8
WCS7	55.34	−26.5	−26.6	n.a.	n.a.
Latest Paleocene	56.04	−26.3	−26.2	−25.8	−29.1
Honeycombs	56.1	−27.2	−27	−26.7	−24
Cf-1	57.39	−26.3	−25.9	−26.6	−24.1
Belt Ash	59.39	−25.8	−26.1	−27	−23.1
Grimy Gulch	63	−27.2	−27.3	−26.5	−24.5

marily derived from angiosperms (Diefendorf et al., 2011; Bush and McInerney, 2013). In contrast, $\delta^{13}C_{leaf}$ calculated from *n*-C_{29} alkane and diterpenoids differed by 2.1‰ ($n = 25$, Wilcoxon Signed Rank, $p < 0.001$), and were similarly different between di- and triterpenoids (1.9‰, $n = 14$, Wilcoxon Signed Rank, $p = 0.04$). These differences in $\delta^{13}C_{leaf}$ are consistent with differences observed between angiosperms and conifers currently living at sites with similar climate (Diefendorf et al., 2010). Leaf $\delta^{13}C$ values calculated from *n*-C_{29} alkanes correlated with bulk $\delta^{13}C$ values when averaged at the site level and the Grimy Gulch site is removed ($R^2 = 0.58$, $p = 0.046$).

3.5. Leaf fractionation in the past

Δ_{leaf} values were calculated using Equation (1) with $\delta^{13}C_{leaf}$ values (determined as noted above from lipids; $\Delta_{leaf\text{-}lipid}$) and $\delta^{13}C_{atm}$ values reconstructed by Tipple et al. (2010). Tipple et al. (2010) calculated $\delta^{13}C_{atm}$ values using planktonic and benthic foraminifera $\delta^{13}C$ and $\delta^{18}O$ records, corrected for temperature-sensitive equilibrium and non-equilibrium isotope effects between carbonate minerals and atmospheric CO_2. Following the suggestions of Tipple et al., in this study, $\delta^{13}C_{atm}$ values from benthic foraminifera were averaged using a 3 million year window. Total uncertainty in the calculated $\Delta_{leaf\text{-}lipid}$ values was determined for each stratigraphic bed using the Monte Carlo method (Anderson, 1976). This approach employs the standard deviations in $\delta^{13}C$ values of the lipids measured within a stratigraphic bed, the uncertainty in ε_{lipid}, and the uncertainty in $\delta^{13}C_{atm}$ values (reported in Tipple et al., 2010), and provides an estimate of their combined influence on net uncertainty using a resampling model. $\Delta_{leaf\text{-}lipid}$ values and associated uncertainty are presented in Table 5 and Fig. 5 with Δ_{leaf} values split by taxonomic group with the assumption that all *n*-alkanes are from angiosperms (Diefendorf et al., 2011).

For *n*-C_{29} alkane, calculated $\Delta_{leaf\text{-}lipid}$ values ranged between 21.2‰ at Dorsey Creek Fence and 23.1‰ at the Honeycombs. Uncertainties in $\Delta_{leaf\text{-}lipid}$ ranged from 2.3 to 2.6‰ (1σ). A one-at-a-time sensitivity analysis was performed to determine the greatest source of uncertainty from *n*-C_{29} alkane. The ε_{lipid} uncertainty explained the greatest amount of the total uncertainty (∼75%) in the Monte Carlo analysis. The remaining uncertainty was split between $\delta^{13}C_{atm}$ and the $\delta^{13}C$*n*-alkanes. $\Delta_{leaf\text{-}lipid}$ values from *n*-C_{31} alkanes and triterpenoids were very similar. However, the uncertainty from the triterpenoids was smaller (1.3 to 1.8‰) and this can be attributed to the smaller uncertainty in triterpenoid ε_{lipid} values. The $\Delta_{leaf\text{-}lipid}$ values for the conifer diterpenoids were lower than $\Delta_{leaf\text{-}lipid}$ values calculated for the angiosperms, with the exception of the Latest Paleocene Honeycombs bed, which has a $\Delta_{leaf\text{-}lipid}$ value of 25.2‰. The mean diterpenoid $\delta^{13}C$ values for each sample at this site are several ‰ more negative than any other stratigraphic bed (Table 3, Fig. 4). More negative $\delta^{13}C$ values were measured in almost all of the tricyclic diterpanes and diterpenes in each of the samples. Interestingly, *n*-alkanes and triterpenoids do not have these negative $\delta^{13}C$ values and are very similar to the beds above and below the Latest Paleocene.

3.6. Leaf fractionation in the past based on modern plants and their sensitivity to water and pCO_2

Leaf fractionation was modeled using Δ_{leaf} estimates generated for a meta-analysis of leaf $\delta^{13}C$ and MAP in living plants (Diefendorf et al., 2010). This modeled Δ_{leaf} ($\Delta_{leaf\text{-}MAP}$) is compared to lipid-based Δ_{leaf} values below. As reported by these and many other authors, Δ_{leaf} values strongly correlate with mean annual precipitation, with the responses of angiosperms' and conifers' Δ_{leaf} values offset by about 2.7‰ (Diefendorf et al., 2010). Thus we used relationships between Δ_{leaf} and water availability for the two major plant types (Eqs. (3), (4); Diefendorf et al., 2010 and discussion therein) to reconstruct predicted values for $\Delta_{leaf\text{-}MAP}$ using proxy-based MAP estimates for each of the Paleogene sites.

Angiosperm modeled $\Delta_{leaf\text{-}MAP}$

$$= 3.14(\pm 0.39) X \log_{10}(MAP) + 11.58(\pm 1.23) \quad (3)$$

Conifer modeled $\Delta_{leaf\text{-}MAP}$

$$= 5.38(\pm 0.76) X \log_{10}(MAP) + 3.16(\pm 2.18) \quad (4)$$

Paleogene MAP values were determined from leaf-area analysis of specimens collected by Currano et al. (2008, 2010) (Table 1). This approach is based on the observation that MAP correlates to the mean natural logarithm of leaf-areas of woody dicotyledon species (Wilf et al., 1998). Paleogene Bighorn Basin MAP values ranged from 109 to 173 cm/year, and the c. 60 cm range in MAP corresponds to modeled $\Delta_{leaf\text{-}MAP}$ values ranging from 21.1 to 21.7‰ and 19.5 to 20.6‰ for angiosperms and conifers, respectively. The effect of elevation on Δ_{leaf}, presumably through reduced atmospheric pressure, has not been included in these calculations, even though modern Δ_{leaf} values were observed to decrease as a function of the square root of elevation (e.g., Diefendorf et al., 2010). The Paleogene paleoelevation changes were likely small, <1 km, although this is poorly constrained (Wing and Greenwood, 1993; McMillan et al., 2006). If all other factors stay equal, then an increase in paleoelevation from 0.5 to 1 km would translate into a Δ_{leaf} decrease of c. 0.5‰ (using the equations reported in Diefendorf et al., 2010), a small change that indicates elevation is not an important factor for this study.

Combined uncertainty in $\Delta_{leaf\text{-}MAP}$ was estimated using the Monte Carlo method based on the modern-plant Δ_{leaf} correlation with MAP (Diefendorf et al., 2010) and from the upper uncertainties for estimated Paleogene MAP (Table 1); combined uncertainties totaled ∼1.9‰ and ∼3.5‰ for angiosperms and conifers, respectively (Table 5). Using a one-at-a-time sensitivity analysis, it was determined that the largest source of error is from the modern Δ_{leaf} calibration. This is likely due to the large ranges in $\delta^{13}C_{leaf}$ for a given MAP observed in Diefendorf et al. (2010). For example,

Table 5
Δ_{leaf} values calculated and modeled from *n*-alkanes, diterpenoids, and triterpenoids for each stratigraphic bed.

Bed name	Age (Ma)	Angiosperms										Conifers			
		Calculated[a]					Modeled					Calculated		Modeled	
		$\Delta_{leaf(n\text{-}C_{29})}$	1σ	$\Delta_{leaf(n\text{-}C_{31})}$	1σ	$\Delta_{leaf\,(triterpenoids)}$	1σ	$\Delta_{leaf\text{-}MAP}$[b]	1σ	$\Delta_{leaf\,pCO_2}$[c]	1σ	Δ_{leaf} Di.	1σ	$\Delta_{leaf\text{-}MAP}$[d]	1σ
Fifteenmile Creek	52.98	21.8	2.3	21.9	2.4	22.0	1.6	21.2	1.9	24.8	3.9	19.5	2.0	19.6	3.5
Dorsey Creek Fence	54.37	21.2	2.3	21.7	2.3	21.3	na	21.4	1.9	22.1	2.6	17.9	na	19.9	3.6
WCS7	55.34	22.1	2.3	22.2	2.3	na	na	21.7	1.9	21.4	2.7	na	na	20.6	3.6
Latest Paleocene	56.04	22.1	2.4	22.1	2.5	21.6	1.3	21.7	2.0	21.5	2.8	25.2	1.9	20.6	3.5
Honeycombs	56.1	23.1	2.4	22.9	2.5	22.6	1.8	21.7	1.9	21.5	2.7	19.8	2.8	20.6	3.5
Cf-1	57.39	22.7	2.4	22.3	2.8	23.0	na	21.1	1.9	22.0	2.5	20.3	2.2	19.5	3.5
Belt Ash	59.39	21.6	2.6	21.9	2.4	22.9	1.4	21.2	1.9	23.0	0.2	18.8	2.7	19.7	3.5
Grimy Gulch	63	22.4	2.5	22.4	2.6	21.6	na	21.2	1.9	21.0	0.6	19.5	2.1	19.7	3.5

[a] Calculated Δ_{leaf} values were determined using the Δ_{leaf} equation (Eq. (1)), after correcting lipid $\delta^{13}C$ values for biosynthetic fractionation (ε_{lipid}; Eq. (2); Diefendorf et al., 2011, 2012), and using $\delta^{13}C_{CO_2}$ values from benthic foraminifera (Tipple et al., 2010).
[b] Modeled Δ_{leaf} from the deciduous angiosperm predictive relationship of Diefendorf et al. (2010, Eq. (3)) and MAP estimates reported in Table 1.
[c] $\Delta_{leaf\text{-}pCO_2}$ modeled from Schubert and Jahren (2012) with pCO_2 values reported in Table 1.
[d] Modeled Δ_{leaf} from the conifer predictive relationship of Diefendorf et al. (2010, Eq. (4)) and MAP values reported in Table 1. Uncertainties for all calculated and modeled values were determined using the Monte Carlo method.

several sites in the tropics have a range of ~8‰ within the same forest, despite averaging values for leaves within a species and restricting analyses to sun exposed canopy leaves (Diefendorf et al., 2010). This variability or 'noise' in $\delta^{13}C_{leaf}$ might be attributed to species effects or to small-scale differences in water availability that are not constrained by climate data in the meta analysis. Regardless, this translates into high uncertainty in the $\Delta_{leaf\text{-}MAP}$ for this study.

Modeled $\Delta_{leaf\text{-}MAP}$ values (based on MAP and taxa) were 0.7‰ ($n = 8$, Wilcoxon Signed Rank, $p = 0.016$) and 0.8‰ (n=7, Wilcoxon Singed Rank, $p = 0.048$) higher than those determined from mean lipid-based Δ_{leaf} values calculated from isotope measurements of n-C_{29} alkanes and triterpenoids, respectively, with a 95% confidence interval (CI) of 0.5‰. For the conifers, lipid-based Δ_{leaf} values are not statistically different than the MAP-based modeled conifer $\Delta_{leaf\text{-}MAP}$ values (n =8, Wilcoxon Signed Rank), even when the Latest Paleocene sample is excluded. However, the range in differences is high (95% CI = 0.5 to −1.6‰; Latest Paleocene excluded) and the $\Delta_{leaf\text{-}MAP}$ uncertainty is also high.

Schubert and Jahren (2012) identified a hyperbolic relationship between Δ_{leaf} and pCO_2 for two herbaceous angiosperm species grown in well-watered chambers over single generations. For comparison, we calculated Δ_{leaf} values as a function of pCO_2 (Fig. 5, Table 5) using Equation (6) reported in Schubert and Jahren (2012) and refer to this as $\Delta_{leaf\text{-}pCO_2}$. Their Equation (6) was based on a compilation of similar studies of that reported pCO_2 effects on Δ_{leaf}, albeit after excluding studies that were not indicative of positive changes in Δ_{leaf} with increasing pCO_2. $\Delta_{leaf\text{-}pCO_2}$ values for angiosperms used pCO_2 values reported in Beerling and Royer (2011) with means calculated for a 4 million-year time step. Reconstructed pCO_2 levels varied between 361 and 946 ppmV (Table 1) with the highest values at the time of deposition of the Eocene Fifteenmile Creek bed. Because of the reconstructed rise in pCO_2 between 53 and 51 Ma, estimates of pCO_2 uncertainty were greater for Fifteenmile Creek than other sites. The closest proxy-based estimate for pCO_2 at this time is 814 ± 240 ppmV at 53.4 Ma (Beerling and Royer, 2011), which is similar to the mean pCO_2 value used here. Reported uncertainty in $\Delta_{leaf\text{-}pCO_2}$ was determined with the Monte Carlo method with the uncertainties in pCO_2 estimated for each stratigraphic bed. This approach results in larger errors at lower pCO_2 because the relationship between Δ_{leaf} and pCO_2 has the greatest slope at low pCO_2, thus small changes in pCO_2 result in large changes in Δ_{leaf}. The uncertainty does not include errors for the parameters of the hyperbolic equation in the report by Schubert and Jahren (2012), who did not report the relationship explicitly. Predicted $\Delta_{leaf\text{-}pCO_2}$ values varied between 21.0 and 24.8, with the highest values at Fifteenmile Creek and Belt Ash (Fig. 5, Table 5).

4. Discussion

4.1. Leaf carbon isotopes based on fossil lipids

Lipid $\delta^{13}C$ values, when converted to leaf $\delta^{13}C$ values, allow us to compare $\Delta_{leaf\text{-}lipid}$ for different major plant taxonomic groups. This approach also enables estimates to be employed for comparison with other carbon archives in isotope-based dietary or soil studies. The range in the fractionation associated with lipid biosynthesis, ε_{lipid}, can be large among species grown under similar climates, and it is currently not well known whether it differs for individual taxa grown under different conditions. Factors such as fixation pathway, growth form, and leaf lifespan are known to be important (Diefendorf et al., 2011, 2012; Magill et al., 2013). However, at present, no systematic study has elucidated environmental or taxonomic controls on ε_{lipid}, specifically as a function of climate, timing of synthesis, and phylogeny. For this study, we

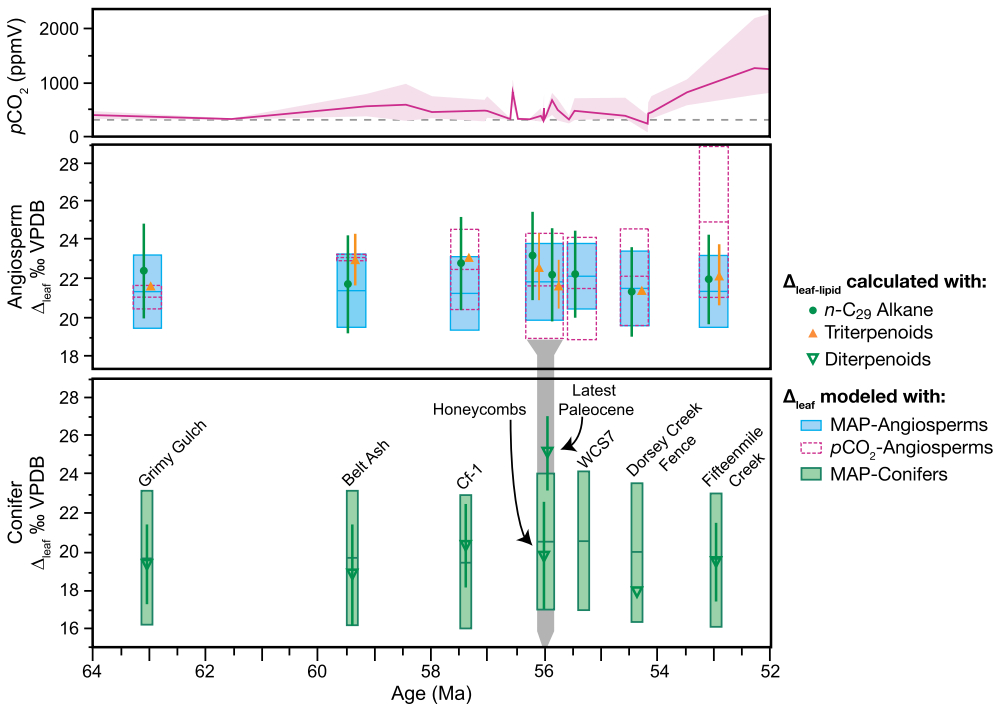

Fig. 5. Carbon isotope fractionation (Δ_{leaf}) separated by conifer and angiosperm taxonomic groups and C) pCO_2 estimates from Beerling and Royer (2011) and present-day pCO_2 indicated with a dashed line. Symbols (circles or triangles) denote mean calculated $\Delta_{leaf\text{-}lipid}$ values for a stratigraphic bed as measured for n-C_{29} alkanes, triterpenoids or diterpenoids. Vertical lines are total uncertainties (1σ) in the calculated $\Delta_{leaf\text{-}lipid}$. Shaded boxes are the modeled Δ_{leaf} values from the modern Δ_{leaf} calibrations based on mean annual precipitation (MAP) with the central horizontal line indicating the mean and the shaded area indicating the total uncertainty (1σ). Dashed boxes indicate the modeled Δ_{leaf} values as a function of atmospheric pCO_2 from Schubert and Jahren (2012) with the central horizontal line indicating the mean and uncertainty shown by the outer box. All samples and boxes were widened relative to their absolute age (Table 1) for visual representation on this figure (i.e. alkane and angiosperm values were separated in time to remove overlap). The Latest Paleocene (56.04 Ma) and the Honeycombs (56.1 Ma) beds were additionally graphically separated to improve visual presentation and are denoted by the grey box at 56 Ma.

used values from Diefendorf et al. (2011, 2012) because: 1) species were chosen specifically in these studies as nearest living relatives to Bighorn Basin species, and 2) species were all grown under similar climatic conditions. Other fractionation factors exist, especially in the tropics (see Magill et al., 2013) and we acknowledge that future studies will revise n-alkane ε_{lipid} values.

Despite current limitations in the state of knowledge regarding ε_{lipid}, we are encouraged by several patterns that emerge from our dataset. For example, lipid-based leaf $\delta^{13}C$ values from n-C_{29}, n-C_{31} alkanes and triterpenoids were similar, which suggests ε_{lipid} values from modern calibrations provide consistent leaf $\delta^{13}C$ values for angiosperms in the Paleogene. Also, calculated conifer $\delta^{13}C_{leaf}$ values are c. 2‰ higher than angiosperms, consistent with comparisons of conifers and angiosperms growing under similar conditions (e.g., Diefendorf et al., 2010).

The range in calculated $\delta^{13}C_{leaf}$ values across a stratigraphic bed is remarkably small (±0.5‰, 1σ) given the range of factors that are known to vary and influence leaf $\delta^{13}C$ values. This low spatial variability in $\delta^{13}C_{n\text{-alkanes}}$ and thus $\delta^{13}C_{leaf}$ is perhaps due to ecological and geologic processes that integrate ecological variability through time and space, such as litter flux, sedimentary transport or the dominance of organic inputs by relatively few, abundant plant species (Graham et al., 2014). In this study, all sites reflect wet floodplain deposition, but TOC and lithology do indeed vary across a stratigraphic bed. The differences in sediment and flora along a bed may reflect patches of slightly better or worse drainage, or other local factors. Perhaps the variation in TOC and lithology reflects variation in redox conditions that are a function of soil depth, soil texture, or flooding frequency across the stratigraphic beds, rather than variability in water that is available to plants, as water was likely abundant. The presence and abundance of plant species and taxonomic groups (e.g. angiosperms and conifers) also typically varies across stratigraphic beds (Davies-Vollum and Wing, 1998), which could give rise to spatial variability in $\delta^{13}C_{n\text{-alkanes}}$ because species with different growth forms, phylogeny, and traits (e.g. leaf lifespan) can differ by as much as 8‰ with respect to Δ_{leaf} even when they grow in the same location (Bonal et al., 2000; Diefendorf et al., 2010). Yet, lipids such as alkanes that are preserved in geologic sediments are almost certainly derived from multiple plant species and multiple generations of plant individuals, and the $\delta^{13}C$ values of preserved lipids are likely weighted toward species that produce more leaves and/or leaf waxes (Graham et al., 2014; Diefendorf et al., 2011). Thus, the $\delta^{13}C$ value of the preserved lipid pool can be thought of as an "average" $\delta^{13}C$ value of the lipid inputs, albeit weighted toward plant species that are more abundant through time and space; this also serves to reduce variability of $\delta^{13}C_{n\text{-alkanes}}$ across a stratigraphic bed. Finally, taphonomic processes (i.e. Ellis and Johnson, 2013) may also be important in filtering for certain species and/or leaf sources (canopy versus understory, etc.), but taphonomic effects on the preservation of leaf waxes in geologic sediments have not been well-studied.

4.2. Modern Δ_{leaf} and ε_{lipid} calibrations as proxies for paleo-Δ_{leaf}

We have attempted to compare Δ_{leaf} values calculated using lipid biomarkers with those modeled using paleoprecipitation. For lipid-based estimates, $\Delta_{leaf\text{-}lipid}$ values varied no more than 2‰ across the eight stratigraphic beds over c. 10 million years of time (Fig. 5). The lipid-based values are in strong agreement with those modeled from MAP despite large changes in temperature (11.7 °C), precipitation (640 mm/yr), and atmospheric $\delta^{13}C$ (1.5‰) during the early Paleogene. Therefore, we argue that lipid biomarkers can be useful, when constrained by precipitation and taxonomic

information, for reconstructing changes in the terrestrial and atmospheric carbon pools in the past.

Although angiosperm data from different lipids were coherent overall, calculated $\Delta_{\text{leaf-lipid}}$ values are slightly higher, by 0.7‰ on average, than modeled Δ_{leaf} values that take into account precipitation. It is however important to note that this difference is smaller than calculated uncertainties. Given the similarity in angiosperm $\delta^{13}C_{\text{leaf}}$ values calculated for *n*-alkanes and triterpenoids, it is unlikely that $\varepsilon_{\text{lipid}}$ values are responsible for the offset. The largest offsets between alkane and triterpenoid–based estimates and those based on MAP were for samples representing 63, 57.39, and 56.1 Ma. These times coincide with the lowest and highest $\delta^{13}C_{\text{atm}}$ values, suggesting that the offset does not reflect changes in $\delta^{13}C_{\text{atm}}$. The observed offsets could reflect the differential influence of poorly constrained factors, such as paleo-MAT, paleo-MAP, paleo-pCO_2 or the modern relationship between Δ_{leaf} and MAP.

Estimates of paleo-MAP for this study were made from leaf area (Wilf et al., 1998), a method with high error. Further, large fossil leaves are not easily preserved and are difficult to recover, which may lead leaf area analyses to underestimate paleo-MAT.

Average annual temperature changed by up to 12 °C in the Bighorn Basin during the Paleogene. The effects of temperature in modern studies of Δ_{leaf} are conflicting (Körner et al., 1991; Diefendorf et al., 2010), potentially because leaves fix most of their carbon within a narrow range of temperature (21.4 ± 2.2 °C) despite a wide range of ambient temperatures (Helliker and Richter, 2008). We find lipid-calculated Δ_{leaf} values do not covary with paleotemperature, suggesting temperature does not account for differences between lipid and MAP-based fractionation reconstructions.

Evidence for the effect of pCO_2 on Δ_{leaf} has been unclear (e.g., Körner et al., 1991; Ehleringer and Cerling, 1995; Polley et al., 1995), potentially because most studies have evaluated short-term pCO_2 effects on Δ_{leaf} (Beerling and Royer, 2002; Franks and Beerling, 2009) and water availability is often unconstrained (Körner, 2007). Schubert and Jahren (2012) identified a relationship between Δ_{leaf} and pCO_2 in well-watered chambers for plants grown over single generations. We used this Δ_{leaf} pCO_2 relationship for our CO_2-based modeled leaf fractionation values ($\Delta_{\text{leaf-}pCO_2}$). Although for some samples, $\Delta_{\text{leaf-}pCO_2}$ agreed nicely with lipid-based Δ_{leaf}, overall, $\Delta_{\text{leaf-}pCO_2}$ differed significantly from $\Delta_{\text{leaf-lipid}}$. For Fifteenmile Creek and Belt Ash stratigraphic beds, high pCO_2 estimates led to the highest modeled $\Delta_{\text{leaf-}pCO_2}$ values. If pCO_2 were a major control on Δ_{leaf} on these timescales, these two wet-depositional sites should have had the highest $\Delta_{\text{leaf-lipid}}$ values, but that was not the case. Although pCO_2, and especially geologically brief fluctuations in pCO_2, are poorly constrained for this time period, this discrepancy suggests it is premature to use modern $pCO_2 - \Delta_{\text{leaf}}$ calibrations to extrapolate to the past, such as for calculating pCO_2.

On short timescales, plants adjust their physiology to optimize leaf gas exchange through stomatal control (Lammertsma et al., 2011). However, on greater than decadal timescales, plants evolve in response to changing pCO_2 by adjusting optimal stomatal size and density and by regulating the rate of carbon fixation to maintain optimal set points, including internal to external CO_2 concentrations (C_i/C_a) (Woodward, 1987; Ehleringer and Cerling, 1995; Woodward and Kelly, 1995; Franks and Beerling, 2009; Franks et al., 2014). Lammertsma et al. (2011) suggested that to study the influence of pCO_2 on plants, plant specimens must exhibit structural adaptation. In fact, several studies that have focused on long-term changes (>100 years) on stomatal conductance and Δ_{leaf} have observed a small decrease in Δ_{leaf} as pCO_2 increases (Penuelas and Azconbieto, 1992; Bert et al., 1997; Duquesnay et al., 1998; Saurer et al., 2004), exactly opposite of $\Delta_{\text{leaf-}pCO_2}$ patterns predicted by Schubert and Jahren (2011). This may not be surprising given that fossil $\delta^{13}C$ values over long periods of Earth history are rather consistent (Deines, 1980; Peters-Kottig et al., 2006), which suggests small changes in C_i/C_a (Franks et al., 2014), despite large changes in pCO_2 (Berner and Kothavala, 2001). The stability of terrestrial plant carbon isotope values over geologic time thus may indicate that optimum Δ_{leaf} values are maintained on long geologic timescales, as suggested by Ehleringer and Cerling (1995). Thus, results from growth chambers must be used cautiously with respect to geologic interpretations, particularly for plant characteristics that likely evolve on timescales longer than one generation (e.g. Δ_{leaf} responsiveness to pCO_2).

4.3. Uncertainties and implications for the geologic record

Modern studies of carbon isotope fractionation during photosynthesis and biomarker synthesis can provide a foundation to account for the competing influences of climate, lipid biosynthesis, and taxonomic group when interpreting changes in Δ_{leaf} based on lipid $\delta^{13}C$ values in the past. However, the uncertainties on $\Delta_{\text{leaf-lipid}}$ in the past are high (±2‰) because of the variability in modern Δ_{leaf} and $\varepsilon_{\text{lipid}}$ values. If these sources of uncertainty are applicable to the geologic record and are representative of a forest, then the Δ_{leaf} range observed in modern forests (e.g., Bonal et al., 2000; Diefendorf et al., 2010) should be considered as a very conservative starting point for estimating the possible uncertainty in geologic $\delta^{13}C$ records. This would require that all studies take modern Δ_{leaf} variability into account when interpreting variation in $\delta^{13}C$ values of organic matter in geologic and modern sediments, at least as a first order approximation of the uncertainty. As mentioned above, variability in the stratigraphic beds studied here is much smaller than the range observed in a single forest (Bonal et al., 2000), either because the variability is small for $\delta^{13}C$ values of organic matter that is delivered to sediments (generally 50% or more carbon in forest litter is from leaves; Graham et al., 2014) or processes reduce the variability, such as time averaging, spatial averaging, or taphonomic effects. Combined, factors that reduce variability may also reduce uncertainty, but future studies will need to determine if that is the case. Nonetheless, on larger spatial scales or over time, variations in $\delta^{13}C$ values will be caused by changes in climate and taxonomic group through their pervasive influences on Δ_{leaf} and $\varepsilon_{\text{lipid}}$. Corrections for these controlling factors must be made to interpret $\delta^{13}C$ values in terrestrial sediments for bulk or lipid-based approaches. For example, if $\delta^{13}C$ values of *n*-alkanes are to be used to interpret changes in water use efficiency through time, then the effect of changing taxonomic group (controls on Δ_{leaf} and $\varepsilon_{\text{lipid}}$) and $\delta^{13}C_{\text{atm}}$ must be removed, or at least ruled out as a control, to realistically interpret $\delta^{13}C$ values of *n*-alkanes.

Using the approach described above, we find that over a 10 million year period marked by substantial climatic changes, calculated $\Delta_{\text{leaf-lipid}}$ values were similar to modeled $\Delta_{\text{leaf-MAP}}$ values (based on paleoprecipitation and the relationship between Δ_{leaf} of living plants and precipitation). The measured uncertainties placed on both calculated $\Delta_{\text{leaf-lipid}}$ and modeled $\Delta_{\text{leaf-MAP}}$ are similar in magnitude and, importantly, the predicted range of values overlap (Fig. 5). Nonetheless, the measured uncertainties are large and can most likely be attributed to the biological variability in modern $\varepsilon_{\text{lipid}}$ and $\Delta_{\text{leaf-MAP}}$. To reduce this biological variability, more systematic studies of the influences of climate, species/phylogeny, growth form, and timing of synthesis on $\varepsilon_{\text{lipid}}$ and Δ_{leaf} are required to determine the best $\varepsilon_{\text{lipid}}$ and Δ_{leaf} values to use for geologic studies. One of the challenges is designing studies with one independent variable to evaluate the effect on fractionation. For example, studying the influence of precipitation on $\varepsilon_{\text{lipid}}$ and Δ_{leaf} requires a precipitation gradient where all other factors, including species, are held constant or otherwise reasonably accounted

for (e.g. using multivariate statistical approaches). The former approach is difficult because there is tremendous species turnover across precipitation gradients.

When interpreting changes in $\delta^{13}C$ records, the influence of climate on ε_{lipid} and Δ_{leaf} is likely most important during carbon isotope excursions (CIEs), such as occurred during the Paleocene–Eocene Thermal Maximum (PETM). Based on a recent review by McInerney and Wing (2011), the range in terrestrial CIEs during the PETM is large, from −2.2 to −7.6‰. Reconciling the magnitude of these terrestrial CIEs has been challenging for many reasons (see McInerney and Wing, 2011). The degree to which the range in CIEs recorded by plant biomarkers is caused by changes in ε_{lipid} and Δ_{leaf} is unclear, but to our knowledge, no studies have estimated the uncertainties in CIEs due to changes in Δ_{leaf} or ε_{lipid}. Other factors, such as pCO_2, may be important controls on fractionation in general (Schubert and Jahren, 2012) and for the PETM (Schubert and Jahren, 2013), but it is unclear if the rate of change at the onset of the PETM is too fast for plants to evolve and acclimate to higher pCO_2.

5. Conclusions

Plant lipid $\delta^{13}C$ values were measured from eight stratigraphic beds in the Bighorn Basin from 63 to 53 Ma. We found that calculated $\delta^{13}C_{leaf}$ values were similar for angiosperm-specific lipids (*n*-alkanes, triterpenoids), indicating that Paleogene ε_{lipid} values for *n*-alkanes and triterpenoids were similar to modern values. Also, $\delta^{13}C_{leaf}$ values calculated from conifer diterpenoids were 2‰ higher than angiosperm values and this is similar to the expected offset for modern angiosperms and conifers grown under the same climate (e.g., Diefendorf et al., 2010).

We found that calculated and modeled $\Delta_{leaf\text{-}MAP}$ values were similar, although offset by ∼0.7‰. The ability to model paleo-Δ_{leaf} values using modern relationships with precipitation suggests that $\Delta_{leaf\text{-}lipid}$ of Paleogene plants was shaped by water availability, major taxonomic group, and biosynthetic fractionation in a manner similar to living plants. If the modern data were not applicable to the past for some reason, then our modeled $\Delta_{leaf\text{-}MAP}$ values would likely not correspond to calculated $\Delta_{leaf\text{-}lipid}$ values as well as they do. The small observed offset could be caused by several factors, but importantly the offset is relatively consistent, suggesting a common factor. In order to better interpret $\delta^{13}C$ values in the geological past, future studies must determine what causes the large variability in modern Δ_{leaf} and ε_{lipid}.

Two stratigraphic beds represent times when pCO_2 levels are thought to have been higher than today. These beds did not have elevated calculated $\Delta_{leaf\text{-}lipid}$ values as would be expected based on modern growth chamber studies, supporting the idea that Δ_{leaf} is insensitive to pCO_2 when plants have sufficient time to acclimate to pCO_2. If changes in stomatal size and density are any indicator, then changes in pCO_2 must be longer than a decade for the long-term effect on Δ_{leaf} to be observed (e.g., Lammertsma et al., 2011). Therefore growth chamber studies may be of limited utility and future studies of CO_2 effects on Δ_{leaf} should focus on plants that have adapted to pCO_2 changes over longer timescales. We show here that, with careful consideration of factors such as paleoprecipitation and reconstructed atmospheric $\delta^{13}C$ values, the $\delta^{13}C$ values of plant biomarkers in geologic sediments might offer a promising tool of evaluating the effects of past changes in pCO_2 on leaf physiology.

Acknowledgements

We thank Francesca McInerney and Dana Royer for their thoughtful reviews. This research was supported by the National Science Foundation (NSF) Grants EAR-0844212 (K.H.F.) and EAR-1229114 (A.F.D.), fellowship awards from the Penn State Biogeochemical Research Initiative for Education (BRIE) funded by NSF IGERT Grant DGE-9972759, an American Chemical Society PRF Grant #51787-DNI2 (A.F.D.), and the Roland W. Brown Fund of the Smithsonian Institution (E.D.C).

Appendix A. Supplementary material

Supplementary material related to this article can be found online at http://dx.doi.org/10.1016/j.epsl.2015.07.029.

References

Anderson, G.M., 1976. Error propagation by the Monte Carlo method in geochemical calculations. Geochim. Cosmochim. Acta 40, 1533–1538.
Beerling, D.J., Royer, D.L., 2002. Fossil plants as indicators of the Phanerozoic global carbon cycle. Annu. Rev. Earth Planet. Sci. 30, 527–556.
Beerling, D.J., Royer, D.L., 2011. Convergent Cenozoic CO_2 history. Nat. Geosci. 4, 418–420.
Berner, R.A., Kothavala, Z., 2001. Geocarb III: a revised model of atmospheric CO_2 over Phanerozoic time. Am. J. Sci. 301, 182–204.
Bert, D., Leavitt, S.W., Dupouey, J.-L., 1997. Variations of wood $\delta^{13}C$ and water-use efficiency of Abies alba during the last century. Ecology 78, 1588–1596.
Bonal, D., Sabatier, D., Montpied, P., Tremeaux, D., Guehl, J.M., 2000. Interspecific variability of $\delta^{13}C$ among trees in rainforests of French Guiana: functional groups and canopy integration. Oecologia 124, 454–468.
Bowen, G.J., 2013. Up in smoke: a role for organic carbon feedbacks in Paleogene hyperthermals. Glob. Planet. Change 109, 18–29.
Bown, T.M., 1980. The Willwood Formation (lower Eocene) of the southern Bighorn Basin, Wyoming, and its mammalian fauna. In: Gingerich, P.D. (Ed.), Early Cenozoic Paleontology and Stratigraphy of the Bighorn Basin, Wyoming, 1880–1980. In: Univ. Michigan Pap. Paleontol., vol. 24, pp. 127–138.
Bush, R.T., McInerney, F.A., 2013. Leaf wax *n*-alkane distributions in and across modern plants: implications for paleoecology and chemotaxonomy. Geochim. Cosmochim. Acta 117, 161–179.
Cernusak, L.A., Ubierna, N., Winter, K., Holtum, J.A.M., Marshall, J.D., Farquhar, G.D., 2013. Environmental and physiological determinants of carbon isotope discrimination in terrestrial plants. New Phytol. 200, 950–965.
Currano, E.D., Labandeira, C.C., Wilf, P., 2010. Fossil insect folivory tracks paleotemperature for six million years. Ecol. Monogr. 80, 547–549.
Currano, E.D., Wilf, P., Wing, S.L., Labandeira, C.C., Lovelock, E.C., Royer, D.L., 2008. Sharply increased insect herbivory during the Paleocene–Eocene Thermal Maximum. Proc. Natl. Acad. Sci. USA 105, 1960–1964.
Davies-Vollum, K.S., Wing, S.L., 1998. Sedimentological, taphonomic, and climatic aspects of Eocene swamp deposits (Willwood Formation, Bighorn Basin, Wyoming). Palaios 13, 28–40.
Deines, P., 1980. The isotopic composition of reduced organic carbon. In: Fritz, P., Fontes, J.C. (Eds.), Handbook of Environmental Isotope geochemistry. Elsevier, Amsterdam, pp. 329–406.
Diefendorf, A.F., Freeman, K.H., Wing, S.L., 2012. Distribution and carbon isotope patterns of diterpenoids and triterpenoids in modern temperate C_3 trees and their geochemical significance. Geochim. Cosmochim. Acta 85, 342–356.
Diefendorf, A.F., Freeman, K.H., Wing, S.L., 2014. A comparison of terpenoid and leaf fossil vegetation proxies in Paleocene and Eocene Bighorn Basin sediments. Org. Geochem. 71, 30–42.
Diefendorf, A.F., Freeman, K.H., Wing, S.L., Graham, H.V., 2011. Production of *n*-alkyl lipids in living plants and implications for the geologic past. Geochim. Cosmochim. Acta 75, 7472–7485.
Diefendorf, A.F., Mueller, K.E., Wing, S.L., Koch, P.L., Freeman, K.H., 2010. Global patterns in leaf ^{13}C discrimination and implications for studies of past and future climate. Proc. Natl. Acad. Sci. USA 107, 5738–5743.
Duquesnay, A., Bréda, N., Stievenard, M., Dupouey, J.L., 1998. Changes of tree-ring $\delta^{13}C$ and water-use efficiency of beech (*Fagus sylvatica L.*) in north-eastern France during the past century. Plant Cell Environ. 21, 565–572.
Ehleringer, J.R., Cerling, T.E., 1995. Atmospheric CO_2 and the ratio of intercellular to ambient CO_2 concentrations in plants. Tree Phys. 15, 105–111.
Ellis, B., Johnson, K.R., 2013. Comparison of leaf samples from mapped tropical and temperate forests: implications for interpretations of the diversity of fossil assemblages. Palaios 28, 163–177.
Farquhar, G.D., Ehleringer, J.R., Hubick, K.T., 1989. Carbon isotope discrimination and photosynthesis. Annu. Rev. Plant Physiol. Plant Mol. Biol. 40, 503–537.
Franks, P.J., Beerling, D.J., 2009. CO_2 forced evolution of plant gas exchange capacity and water-use efficiency over the Phanerozoic. Geobiology 7, 227–236.
Franks, P.J., Royer, D.L., Beerling, D.J., Van de Water, P.K., Cantrill, D.J., Barbour, M.M., Berry, J.A., 2014. New constraints on atmospheric CO_2 concentration for the Phanerozoic. Geophys. Res. Lett. 41, 2014GL060457.
Freeman, K.H., Mueller, K.E., Diefendorf, A.F., Wing, S.L., Koch, P.L., 2011. Clarifying the influence of water availability and plant types on carbon isotope discrimination by C3 plants. Proc. Natl. Acad. Sci. USA 108, E59–E60.

Graham, H.V., Patzkowsky, M.E., Wing, S.L., Parker, G.G., Fogel, M.L., Freeman, K.H., 2014. Isotopic characteristics of canopies in simulated leaf assemblages. Geochim. Cosmochim. Acta 144, 82–95.

Hayes, J.M., 2001. Fractionation of carbon and hydrogen isotopes in biosynthetic processes. Rev. Mineral. Geochem. 43, 225–277.

Helliker, B.R., Richter, S.L., 2008. Subtropical to boreal convergence of tree-leaf temperatures. Nature 454, 511–514.

Jones, H.L., Hajek, E.A., 2007. Characterizing avulsion stratigraphy in ancient alluvial deposits. Sediment. Geol. 202, 124–137.

Kolattukudy, P., Croteau, R., Buckner, J., 1976. Biochemistry of plant waxes. In: Kolattukudy, P. (Ed.), Chemistry and Biochemistry of Natural Waxes. Elsevier, Amsterdam, pp. 289–347.

Körner, C., 2007. The use of 'altitude' in ecological research. Trends Ecol. Evol. 22, 569–574.

Körner, C.H., Farquhar, G.D., Wong, S.C., 1991. Carbon isotope discrimination by plants follows latitudinal and altitudinal trends. Oecologia 88, 30–40.

Lammertsma, E.I., Boer, H.J.d., Dekker, S.C., Dilcher, D.L., Lotter, A.F., Wagner-Cremer, F., 2011. Global CO_2 rise leads to reduced maximum stomatal conductance in Florida vegetation. Proc. Natl. Acad. Sci. USA 108, 4035–4040.

Magill, C.R., Ashley, G.M., Freeman, K.H., 2013. Ecosystem variability and early human habitats in eastern Africa. Proc. Natl. Acad. Sci. USA 110, 1167–1174.

McInerney, F.A., Wing, S.L., 2011. The Paleocene–Eocene thermal maximum: a perturbation of carbon cycle, climate, and biosphere with implications for the future. Annu. Rev. Earth Planet. Sci. 39, 489–516.

McMillan, M.E., Heller, P.L., Wing, S.L., 2006. History and causes of post-Laramide relief in the Rocky Mountain orogenic plateau. Geol. Soc. Am. Bull. 118, 393–405.

Penuelas, J., Azconbieto, J., 1992. Changes in leaf delta-C-13 of herbarium plant-species during the last 3 centuries of CO_2 Increase. Plant Cell Environ. 15, 485–489.

Peters-Kottig, W., Strauss, H., Kerp, H., 2006. The land plant $\delta^{13}C$ record and plant evolution in the Late Palaeozoic. Palaeogeogr. Palaeoclimatol. Palaeoecol. 240, 237–252.

Polley, H.W., Johnson, H.B., Mayeux, H.S., 1995. Nitrogen and water requirements of C3 plants grown at glacial to present carbon dioxide concentrations. Funct. Ecol. 9, 86–96.

Saurer, M., Siegwolf, R.T.W., Schweingruber, F.H., 2004. Carbon isotope discrimination indicates improving water-use efficiency of trees in northern Eurasia over the last 100 years. Glob. Change Biol. 10, 2109–2120.

Schubert, B.A., Jahren, A.H., 2012. The effect of atmospheric CO_2 concentration on carbon isotope fractionation in C3 land plants. Geochim. Cosmochim. Acta 96, 29–43.

Schubert, B.A., Jahren, A.H., 2013. Reconciliation of marine and terrestrial carbon isotope excursions based on changing atmospheric CO_2 levels. Nat. Commun. 4, 1653.

Tipple, B.J., Meyers, S.R., Pagani, M., 2010. Carbon isotope ratio of Cenozoic CO_2: a comparative evaluation of available geochemical proxies. Paleoceanography 25, PA3202.

Wilf, P., Wing, S.L., Greenwood, D.R., Greenwood, C.L., 1998. Using fossil leaves as paleoprecipitation indicators: an Eocene example. Geology 26, 203–206.

Wing, S.L., 1984. Relation of paleovegetation to geometry and cyclicity of some fluvial carbonaceous deposits. J. Sediment. Petrol. 54, 52–66.

Wing, S.L., Bao, H., Koch, P.L., 2000. An early Eocene cool period? Evidence for continental cooling during the warmest part of the Cenozoic. In: Huber, B.T., MacLeod, K.G., Wing, S.L. (Eds.), Warm Climates in Earth History. Cambridge University Press, New York, pp. 197–236.

Wing, S.L., Currano, E.D., 2013. Plant response to a global greenhouse event 56 million years ago. Am. J. Bot. 100, 1234–1254.

Wing, S.L., Greenwood, D.R., 1993. Fossils and fossil climate: the case for equable continental interiors in the Eocene. Philos. Trans. R. Soc. Lond. B, Biol. Sci. 341, 243–252.

Wing, S.L., Harrington, G.J., Smith, F.A., Bloch, J.I., Boyer, D.M., Freeman, K.H., 2005. Transient floral change and rapid global warming at the Paleocene–Eocene boundary. Science 310, 993–996.

Woodward, F.I., 1987. Stomatal numbers are sensitive to increased CO_2 from pre-industrial levels. Nature 327, 617–618.

Woodward, F.I., Kelly, C.K., 1995. The influence of CO_2 concentration on stomatal density. New Phytol. 131, 311–327.